INTERNATIONAL JOURNAL OF REFRIGERATION 56 (2015) 186–197

Available online at www.sciencedirect.com

ScienceDirect

journal homepage: www.elsevier.com/locate/ijrefrig

Thermodynamic analysis of natural gas reciprocating compressors based on real and ideal gas models

Mahmood Farzaneh-Gord [a], *Amir Niazmand* [a], *Mahdi Deymi-Dashtebayaz* [b], *Hamid Reza Rahbari* [a,*]

[a] *The Faculty of Mechanical Engineering, Shahrood University of Technology, Shahrood, Iran*
[b] *Department of Mechanical Engineering, Hakim Sabzevari University, Sabzevar, Iran*

ARTICLE INFO

Article history:
Received 3 August 2014
Received in revised form
11 November 2014
Accepted 12 November 2014
Available online 24 November 2014

Keywords:
Reciprocating compressor
Natural gas
Thermodynamic modeling
AGA8 equation of state

ABSTRACT

The accurate modelling and investigating effects of various parameters of the reciprocating compressors are important subjects. In this work, based on first law of thermodynamics, conversation of mass and real and ideal gas assumptions, a theoretical analysis has been constructed to simulate natural gas reciprocating compressors. For computing the thermodynamic properties of natural gas based on real gas model, the AGA8 equation of state has been used. Numerical results validated with previous measured values and showed a good agreement. The effects of important parameters such as: angular speed, clearance and pressure ratio have been studied on the performance of the compressors. The results reveal the in-control volume temperature for ideal gas is more than real gas model but the mass flow rate and work for real gas is higher than ideal gas model. On the other hand, the indicated work that required for compression is greater for ideal gas model.

Analyse thermodynamique de compresseurs à piston au gaz naturel basée sur des modèles de gaz réel et idéal

Mots clés : Compresseur à piston ; Gaz naturel ; Modélisation thermodynamique ; Equation d'état AGA8

1. Introduction

One of the most important equipment for producing high pressure gas is reciprocating compressors. These compressors are used widely in industries such as: refineries and power plants, refrigeration system (chillers), Compressed Natural Gas stations (CNG stations) and etc. due to high pressure ratio achievement.

As noted above, the CNG station is one of the most applications of reciprocating compressors. In CNG station, natural gas from the distribution pipeline is compressed using a large multi-stage compressor (three or four stages) to pressure

* *Corresponding author.*
E-mail addresses: mahmood.farzaneh@yahoo.co.uk (M. Farzaneh-Gord), amir_omid86@yahoo.com (A. Niazmand), m.deimi@hsu.ac.ir, meh_deimi@yahoo.com (M. Deymi-Dashtebayaz), rahbarihamidreza@yahoo.com (H.R. Rahbari).
http://dx.doi.org/10.1016/j.ijrefrig.2014.11.008
0140-7007/

Nomenclature

a	lengths of rod m
A	area (m^2)
C_d	orifice discharge coefficient
c_p, c_v	Constant pressure &volume specific heats (kJ kg^{-1} K^{-1})
g	Gravitational acceleration (m s^{-2})
h	Specific enthalpy (kJ kg^{-1})
L	crank m
$\dot{m}$	Mass flow rate (kg s^{-1})
M	Molecular weight (kg $kmol^{-1}$)
P	Pressure (bar or Pa)
$\dot{Q}$	Heat transfer rate (kW)
S	stroke m
T	Temperature (K or °C)
u	internal energy (kJ kg^{-1})
v	specific volume (m^3 kg^{-1})
V	Volume (m^3)
V_0	Dead Volume (m^3)
v	Velocity (m s^{-1})
W	Actual work (kJ kg^{-1})
$\dot{W}$	Actual work rate (kW or MW)
x	displacement (m)
z	Height (m)
ρ	Density (kg m^{-3})
ω	Angular Speed (rad s^{-1})
α	Heat Transfer Coefficient (Wm^2/K)
θ	Degree (Degree)

Subscript

cv	Control Volume
s	Suction
d	discharge
p	piston

between 20 MPa and 25 MPa (Farzaneh-Gord et al., 2014, 2012). A large part of the initial and current costs of CNG stations are due to reciprocating compressor input work (Farzaneh-Gord et al., 2012). By modeling CNG compressors, one could optimize design parameters which lead to higher efficiency and lower input work for compressing in CNG stations.

Researchers have used different methods for modeling reciprocating compressor. These methods usually divided into two methods: global models and differential models, that in these methods the variable depends on crank angle (Stouffs et al., 2000). Stouffs et al. (2000) with utilizing global model studied reciprocating compressors thermodynamically. In their model five mains and four secondary dimensionless physical parameters were important and they computed the volumetric effectiveness, the work per unit mass and the indicated efficiency. Casting et al. (Castaing-Lasvignottes and Gibout, 2010) modeled compressor operation using performance explanations like volumetric, isentropic and effective. They thought that these efficiencies depend basically on two parameters, the dead volumetric ratio, having particular influence on volumetric efficiency, and a friction factor mainly influencing both isentropic and effective efficiencies. Elhaj et al. (Elhaji et al., 2008) studied a two-stage reciprocating compressor numerically. An important achievement of this research was expansion of diagnostic features for predictive condition monitoring. Winandy et al. (2002) exhibited a simplified model of an open-type reciprocating compressor. Their analysis presented the main processes influenced the refrigerant mass flow rate and the compressor power and the discharge temperature. Also Ndiaye and Bernier (2010) did a dynamic model of a hermetic reciprocating compressor in on-off cycling operation. Also Farzaneh-Gord et al. (2013) optimized design parameters of reciprocating air compressor thermodynamically. They developed a mathematical model according to the mass conservation, first law and ideal gas assumption to study the performance of reciprocating compressors.

All the researchers mentioned above used the first law of thermodynamics for modeling as basic tool. The second law of thermodynamic is also used to analysis performance of the reciprocating compressors. McGovern and Harte (1995) investigated the compressor performance with employing the second law. The non-idealities are characterized as exergy destruction rates as losses to friction, irreversible heat transfer, fluid throttling and irreversible fluid mixing. Defects in the use of a compressor's shaft power identified and quantified. Aprea et al. (2009) presented a research that detected for variable speed compressors the current frequency that optimizes the exergy, energy and economy aspects. Also, Bin et al. (2013) investigated thermal performance of reciprocating compressor with stepless capacity control system. In their research an experimental setup was working and the compressor with designed stepless capacity control system operate all right. Morriesen and Deschamps (2012) investigated transient fluid and superheating in the suction chamber of a refrigeration reciprocating compressor experimentally. Also Yang et al. (2012) simulated a semi-hermetic CO_2 reciprocating compressor comprehensively.

The effects of a few more design parameters on the performance of the compressor have also investigated in various studies. Perez-Segarra et al. (2005) carried out the comprehensive analysis of various famous thermodynamic efficiencies such as the volumetric efficiency, the isentropic efficiency and the combined mechanical-electrical efficiency, which these efficiencies prevalently employed to characterize hermetic reciprocating compressors. They separated these efficiencies into their main components (physical subprocesses). Da Riva and Del Col (2011) introduced the performance of a semi-hermetic reciprocating compressor experimentally. This compressor has been installed in a heat pump for producing 100 kW heating capacity. The effect of the use of an internal heat exchanger between liquid and vapour line on the performance of the compressor is discussed. Damle et al. (2011) studied the simulation that applies an object-oriented unstructured modular methodology for the numerical modeling of the elements forming the hermetic reciprocating compressor domain to predict the thermal and fluid dynamic behavior (temperature, pressure, mass flow rates, power consumption, etc.) of the compressor. Link and Deschamps (2011) investigated a simulation methodology, experimental validated, to study the compressor in transients time. Furthermore, their model is used to appraise the minimum voltage needed for the compressor startup as a function of the

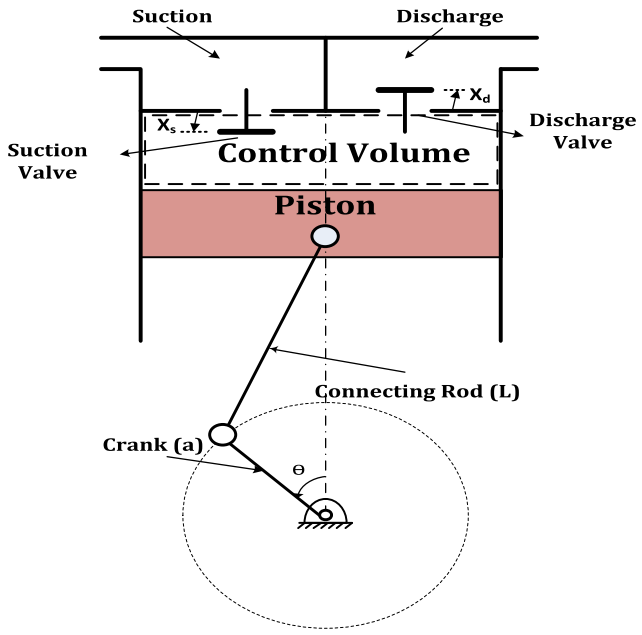

Fig. 1 – Schematic of reciprocating compressor.

equalized pressure and the auxiliary coil actuation time. Cezar et al. (2011) investigated the unsteady behavior of mass flow rate and power of reciprocating compressor based on a semi-empirical numerical simulation. Their simulation is established on thermodynamic equations fitted to manufacturer data by utilizing linear correlations. Ma et al. (2012) was developed a semi-hermetic reciprocating compressor for application in CO_2 refrigeration. The movement of the valve was discussed in detail for the trans-critical CO_2 compressor with the experimental results.

For analysing natural gas reciprocating compressors accurately, it is necessary to know thermodynamic properties of natural gas. One of the most reliable methods for calculating natural gas thermodynamic properties is the AGA8 Equation of State (AGA8–DC92 EoS, 1992; ISO-12213-2, 1997). The AGA8 equation of state has been presented by American Gas Association specifically for computing compressibility factor and density of natural gas. This equation of state has been also subject to different studies in order to compute thermodynamics properties of natural gas (Maríc et al., 2005; Maríc, 2005, 2007; Farzaneh-Gord et al., 2010; Farzaneh-Gord and Rahbari, 2012). Farzaneh-Gord and Rahbari (2012) has employed AGA8 EOS to calculate variety of natural gas thermodynamic properties for various natural gas mixtures.

The improvement of design parameters of CNG reciprocating compressors leads to higher compressor performance. By simulating these compressors, it is possible to investigate effects of different parameters on their efficiency and to recognize the best design parameters. Also by modeling reciprocating compressors, it is possible to diagnosis possible fault which reduce compressor performance.

This study has been enlarged dramatically from above mentioned researches by presenting a detailed numerical methodology for simulating one stage CNG reciprocating compressors. The working fluid is natural gas that its thermodynamic properties are computed based on ideal and real gas assumptions. For real gas model, the thermodynamic properties of natural gas mixture calculated based on AGA8 equation of state. The results from the developed model have been validated against the previous experimental values. The effects of various parameters on the performance of the compressors have been compared between ideal and real gas models. An optimum value for suction to discharge valve area ratio has been introduced for each gas models.

2. Methodology

The schematic diagram of a CNG reciprocating compressor with spring type suction and discharge valves is shown in Fig. 1. The rotary motion of crankshaft is converted to the reciprocating motion of piston by connecting rod. Gas in cylinder is assumed as lump open system. It is assumed that no leakage take place in the compressor. The governing equation for modelling the compressor is introduced in this section.

2.1. First law equation

To present a mathematical model, the continuity and first law of thermodynamics has been used. The cylinder wall, cylinder head and piston end face are considered as boundaries for control volume. The first thermodynamic law is written as follow:

$$\dot{Q}_{cv} + \sum \dot{m}_s \left(h_s + \frac{Ve_s^2}{2} + gz_s \right) = \sum \dot{m}_d \left(h_d + \frac{Ve_d^2}{2} + gz_d \right) + \frac{d}{dt}\left[m\left(u + \frac{Ve^2}{2} + gz \right) \right]_{cv} + \dot{W}_{cv} \quad (1)$$

where $\dot{Q}$, $\dot{m}$, h, Ve, g, z and $\dot{W}$ are heat transfer and mass flow rates, enthalpy, velocity, acceleration of gravity, altitude and work rate respectively. Also s, d and cv subscripts stand for suction, discharge and control volume condition respectively. If variation in kinetic and potential energies are neglected, then this equation could be simplified as follow:

$$\frac{dQ_{cv}}{dt} + \frac{dm_s}{dt} h_s = \frac{dm_d}{dt} h_d + \frac{d}{dt}(mu)_{cv} + \frac{dW_{cv}}{dt} \quad (2)$$

The work rate could be computed as follow:

$$\frac{dW_{cv}}{dt} = P_{cv} \frac{dV_{cv}}{dt} \quad (3)$$

where P and V are pressure and volume respectively. With combining equations (2) and (3), the following equation can be obtained:

$$\frac{dQ_{cv}}{dt} + \frac{dm_s}{dt} h_s = \frac{dm_d}{dt} h_d + \frac{d}{dt}(mu)_{cv} + P_{cv} \frac{dV_{cv}}{dt} \quad (4)$$

Also, differentiating respect to time could be converted to crank angle by considering the following equation:

$$\frac{d}{dt} = \frac{d}{d\theta} \times \frac{d\theta}{dt} = \omega \frac{d}{d\theta} \tag{5}$$

In which, ω is the rotational speed of the crank shaft. Finally the first law thermodynamic equation changed as below:

$$\frac{dQ_{cv}}{d\theta} + \frac{dm_s}{d\theta} h_s = \frac{dm_d}{d\theta} h_d + \frac{d}{d\theta}(mu)_{cv} + P_{cv} \frac{dV_{cv}}{d\theta} \tag{6}$$

2.2. Piston motion equation

The exact expression for the instantaneous position of the piston displacement from top dead center in terms of the crank angle may be given by Lee (1983):

$$x(\theta) = \frac{S}{2}\left[1 - \cos\theta + \frac{L}{a}\left(1 - \sqrt{\left(1 - \left(\frac{a}{L}\sin\theta\right)^2\right)}\right)\right] \tag{7}$$

where a, L and S are lengths of rod and crank and stroke respectively. The momentarily volume of cylinder is obtained by reference (Lee, 1983):

$$V_{cv}(\theta) = A_{cv} \times S(\theta) + V_0 \tag{8}$$

where V_0 is the dead volume.

2.3. Continuity equation

Considering the in-cylinder gas of compressor as a control volume the continuity (conservation of mass) equation may be written as follows:

$$\frac{dm_{cv}}{dt} = \dot{m}_s - \dot{m}_d \tag{9}$$

By replacing equation (5) in equation (9), the quantity equation could be written as:

$$\frac{dm_{cv}}{d\theta} = \frac{1}{\omega}(\dot{m}_s - \dot{m}_d) \tag{10}$$

where $\dot{m}_s$ and $\dot{m}_d$ are the mass flow rate through suction and discharge valves respectively, which are computing from following equations (Brablik, 1972)

$$\dot{m}_s = \begin{cases} C_{ds}\rho_s A_s \sqrt{\dfrac{2(P_s - P_{cv})}{\rho_s}} & \text{for } P_s > P_{cv} \quad \text{and} \quad x_s > 0 \\ -C_{ds}\rho_{cv} A_s \sqrt{\dfrac{2(P_{cv} - P_s)}{\rho_{cv}}} & \text{for } P_{cv} > P_s \quad \text{and} \quad x_s > 0 \end{cases} \tag{11}$$

$$\dot{m}_d = \begin{cases} C_{dd}\rho_{cv} A_d \sqrt{\dfrac{2(P_{cv} - P_d)}{\rho_s}} & \text{for } P_{cv} > P_d \quad \text{and} \quad x_d > 0 \\ -C_{dd}\rho_d A_d \sqrt{\dfrac{2(P_d - P_{cv})}{\rho_d}} & \text{for } P_d > P_{cv} \quad \text{and} \quad x_d > 0 \end{cases} \tag{12}$$

where A_s and A_d are the flow areas through the suction and discharge valves which take place from cylinder respectively. They are obtained by:

$$\begin{aligned} A_s &= 2\pi x_s r_s \\ A_d &= 2\pi x_d r_d \end{aligned} \tag{13}$$

where x_s and x_d are the suction and discharge displacement from the closed position, and, r_s and r_d are radius of suction and discharge valves respectively.

Due to non-ideality of the valve, it does not shut down instantaneously as soon as a negative pressure difference is created from its reference motion, turn the direction and shut the opening. Coefficient of c_{ds} and c_{dd} account these non-ideality of valves.

2.4. Valve movement equation

The valve dynamic equations are derived based on the following assumption;

(i) The valve is considered as a single degree of freedom system.
(ii) The valve plate is rigid.
(iii) The valve displacement is restricted by a suspension device.

Reference point of motion is the closed position of the valve and the valves do not have any negative displacement. Considering the forces acting to the valve plates, the general equation of motion for a valve plate is then given by Singh (1975):

$$\frac{d^2x_s}{d\theta^2} = \frac{1}{m_s\omega^2}\{-k_s\omega_s + C_{fs}A_s(P_s - P_{cv}) + F_{ps}\} \quad \text{for } x_s > 0 \quad \text{and} \quad x_s^{max} > x_s \tag{14}$$

$$\frac{d^2x_d}{d\theta^2} = \frac{1}{m_d\omega^2}\{-k_d\omega_d + C_{fd}A_d(P_{cv} - P_d) + F_{pd}\} \quad \text{for } x_d > 0 \quad \text{and} \quad x_d^{max} > x_d \tag{15}$$

where F_{ps} and F_{pd} are pre-load forces, that these forces are neglected respect to another forces. Also m_s and m_d are masses of suction and discharge, respectively. Coefficient of C_{fs} and C_{fd} account loss of the energy due to the orifice flow and these coefficients can be obtained from Boswirth (1980).

2.5. Heat transfer equation

Heat transfer due to convection in compression chamber can be calculated for each crank angle from equation (16) as:

$$\frac{dQ}{d\theta} = \frac{\alpha A}{\omega}(T_{cv} - T_w) \tag{16}$$

where α, A, T_{cv} and T_w are the heat transfer coefficient, surface area in contact with the gas, the in-cylinder gas temperature and the wall temperature respectively. Adair et al. (1972) observed that the cylinder wall temperature varies less than ±1°F as a result the wall temperature is assumed constant.

To calculate convective heat transfer coefficient, α, the Woschni correlation has been employed (Richard, 1999). This correlation is originally derived for internal combustion engine. The correlation could also predict the heat transfer rate during compression stage of engine motion. Consequently, it could be used to model heat transfer in a reciprocating compressor. According to the correlation, the heat transfer coefficient is given by:

$$\alpha = 3.26D^{-0.2}P^{0.8}T^{-0.55}\upsilon^{0.8} \tag{17}$$

where, υ and D are the characteristic velocity of gas and diameter of the cylinder respectively. According to Woschni correlation, the correlation characteristic velocity for a compressor without swirl is given as (Richard, 1999):

$$\upsilon = 2.28v_p \tag{18}$$

where, v_p is average velocity of piston.

2.6. Ideal gas model

For the case of assuming ideal gas behaviour, the governing equation could be much simplified. Considering the following ideal gas assumptions:

$$u = C_vT,\ h = C_pT\ ,\ C_p - C_v = R,\ PV = mRT \tag{19}$$

Consequently,

$$\frac{d(mu)_{cv}}{d\theta} = m_{cv}C_v\frac{dT_{cv}}{d\theta} + T_{cv}C_v\frac{dm_{cv}}{d\theta} \tag{20}$$

With replacing ideal gas assumptions and equation (16), the equation (6) could be simplified as below:

$$m_{cv}C_v\frac{dT_{cv}}{d\theta} + T_{cv}C_v\frac{dm_{cv}}{d\theta} = U_{(\theta)}A_{cv(\theta)}\left(T_{cv(\theta)} - T_{am}\right) + \dot{m}_sC_pT_s - \dot{m}_dC_pT_d - P_{cv}\frac{dV_{cv}}{d\theta} \tag{21}$$

3. Computing natural gas thermodynamics properties

It is clear that for calculating in-control volume properties, the two independent thermodynamic properties should be computed and then other properties calculated. The two properties are density (or specific volume) and internal energy which calculated from conservation of mass and first law of thermodynamic respectively. The methods for computing thermodynamic properties are presented in this section briefly. The detailed procedure for thermodynamics property calculation could be found in Farzaneh-Gord and Rahbari (2012).

3.1. AGA8 EOS

The general form of AGA8 EOS is defined as follows (AGA8–DC92 EoS, 1992):

$$P = Z\rho_mRT \tag{22}$$

where Z,ρ_m and R are compressibility factor, molar density and universal gas constant respectively.

In AGA8 method, the compressibility factor should be calculated by employing the following equation (AGA8–DC92 EoS, 1992):

$$Z = 1 + B\rho_m - \rho_r\sum_{n=13}^{18}C_n^* + \sum_{n=13}^{18}C_n^*D_n^* \tag{23}$$

where, ρ_r is reduced density and defined as follows:

$$\rho_r = K^3\rho_m \tag{24}$$

where in equation (24), K is mixture size parameter and calculated using following equation (AGA8–DC92 EoS, 1992):

$$K^5 = \left(\sum_{i=1}^{N}x_iK_i^{\frac{5}{2}}\right)^2 + 2\sum_{i=1}^{N-1}\sum_{j=i+1}^{N}x_ix_j\left(K_{ij}^5 - 1\right)\left(K_iK_j\right)^{\frac{5}{2}} \tag{25}$$

In equation (25), x_i is mole fraction of component i in mixture, x_j is mole fraction of component j in mixture, K_i is size parameter of component i, K_j is size parameter of component j, K_{ij} is binary interaction parameter for size and N is number of component in gas mixture.

In equation (23), B is second virial coefficient and given by the following equation (AGA8–DC92 EoS, 1992):

$$B = \sum_{n=1}^{18}a_nT^{-u_n}\sum_{i=1}^{N}\sum_{j=1}^{N}x_ix_jB_{nij}^*E_{ij}^{u_n}\left(K_iK_j\right)^{\frac{3}{2}} \tag{26}$$

where, B_{nij}^* and E_{ij} are defined by the following equations (AGA8–DC92 EoS, 1992):

$$B_{nij}^* = \left(G_{ij}+1-g_n\right)^{g_n}\left(Q_iQ_j+1-q_n\right)^{q_n}\left(F_i^{1/2}F_j^{1/2}+1-f_n\right)^{f_n}\left(S_iS_j+1-s_n\right)^{s_n}\left(W_iW_j+1-w_n\right)^{w_n} \tag{27}$$

$$E_{ij} = E_{ij}^*\left(E_iE_j\right)^{1/2} \tag{28}$$

In equation (27), G_{ij} is defined by the following equation (AGA8–DC92 EoS, 1992):

$$G_{ij} = \frac{G_{ij}^*\left(G_i + G_j\right)}{2} \tag{29}$$

In equations (25)–(29), a_n, f_n, g_n, q_n, s_n, u_n, w_n are the equation of state parameters, E_i, F_i, G_i, K_i, Q_i, S_i,W_i are the corresponding characterization parameters and E_{ij}^*, G_{ij}^* are corresponding binary interaction parameters.

In equation (23), $C_n^*; n = 1, \ldots, 58$ are temperature dependent coefficients and defined by the following equation (AGA8–DC92 EoS, 1992):

$$C_n^* = a_n\left(G+1-g_n\right)^{g_n}\left(Q^2+1-q_n\right)^{q_n}\left(F+1-f_n\right)^{f_n}U_n^{u_n}T^{-u_n} \tag{30}$$

In equation (30),G,F,Q,U are the mixture parameters and defined by the following equations (AGA8–DC92 EoS, 1992):

$$U^5 = \left(\sum_{i=1}^{N}x_iE_i^{\frac{5}{2}}\right)^2 + 2\sum_{i=1}^{N-1}\sum_{j=i+1}^{N}x_ix_j\left(U_{ij}^5 - 1\right)\left(E_iE_j\right)^{\frac{5}{2}} \tag{31}$$

$$G = \sum_{i=1}^{N}x_iG_i + 2\sum_{i=1}^{N-1}\sum_{j=i+1}^{N}x_ix_j\left(G_{ij}^* - 1\right)\left(G_i + G_j\right) \tag{32}$$

$$Q = \sum_{i=1}^{N}x_iQ_i \tag{33}$$

$$F = \sum_{i=1}^{N}x_i^2F_i \tag{34}$$

where in equation (31), U_{ij} is the binary interaction parameter for mixture energy.

In equation (23), D_n^* is defined by the following equation:

$$D_n^* = \left(b_n - c_nk_n\rho_r^{k_n}\right)\rho_r^{k_n}\exp\left(-c_n\rho_r^{k_n}\right) \tag{35}$$

Coefficients of equation (35) are introduced in reference (Damle et al., 2011).

Substituting equation (23) in equation (22), the temperature, pressure and composition of natural gas are known. The only unknown parameter is molar density. The molar density is calculated using Newton–Raphson iterative method.

The density of natural gas is then calculated by the following equation:

$$\rho = M_w \rho_m \tag{36}$$

where, M_w is molecular weight of mixture and ρ_m is molar density. With being known molar density, compressibility factor is calculated using equation (23).

AGA8 model is indented for specific range of the gas components. Table 1 shows range of gas characteristics to which AGA8 EOS model could be employed (AGA8–DC92 EoS, 1992). It shows good performance and high accuracy in the temperature range between 143.15 K and 676.15 K, and for a pressure up to 280 MPa.

3.2. Computing internal energy (u)

Assuming internal energy is a function of temperature and molar specific volume, the internal energy residual function could be calculated as (Moran and Shapiro, 2007):

$$u_m - u_{m,I} = -RT^2 \int_0^{\rho_m} \left(\frac{\partial Z}{\partial T}\right)_{\rho_m} \frac{d\rho_m}{\rho_m} \tag{37}$$

where, u_m is molar internal energy for real gas and $u_{m,I}$ is molar internal energy for ideal gas. Molar internal energy for ideal gas could be calculated using the following equation:

$$u_{m,I} = h_{m,I} - P\nu_m = h_{m,I} - RT \tag{38}$$

In equation (38), $h_{m,I}$ is molar enthalpy for ideal gas and calculated using below equation, T is temperature and R is universal gas constant.

$$h_{m,I} = \sum_{j=1}^{N} x_j {h_{m,i}}^j \tag{39}$$

Table 1 – Range of gas mixture characteristics in AGA8 model (AGA8–DC92 EoS, 1992).

Component (mole %)	Normal range	Expanded range
Methane	45 to 100	0 to 100
Nitrogen	0 to 50	0 to 100
Carbon dioxide	0 to 30	0 to 100
Ethane	0 to 10	0 to 100
Propane	0 to 4	0 to 12
Total butanes	0 to 1	0 to 6
Total pentanes	0 to 0.3	0 to 4
Hexanes plus	0 to 0.2	0 to Dew point
Helium	0 to 0.2	0 to 3
Hydrogen	0 to 10	0 to 100
Carbon monoxide	0 to 3	0 to 3
Argon	0	0 to 1
Oxygen	0	0 to 21
Water	0 to 0.05	0 to Dew point
Hydrogen sulfide	0 to 0.02	0 to 100

Also, the internal energy per unit mass is defined as follows:

$$u = \frac{u_m}{M_w} \tag{40}$$

3.3. Computing enthalpy (h)

One of thermal properties for natural gas is enthalpy. Assuming enthalpy is a function of temperature and molar specific volume, the enthalpy residual function is defined as follows (Moran and Shapiro, 2007):

$$h_m - h_{m,I} = \int_{\upsilon_{m,I}}^{\upsilon_m} \left[T\left(\frac{\partial P}{\partial T}\right)_{\upsilon_m} - P\right] d\upsilon_m + \int_{\upsilon_{m,I}\to\infty}^{\upsilon_m} RT\left(\frac{\partial Z}{\partial \upsilon_m}\right)_T d\upsilon_m \tag{41}$$

In equation (41), h_m is molar enthalpy for real gas, $h_{m,I}$ molar enthalpy for ideal gas and $\upsilon_{m,I}$ is molar specific volume for ideal gas. By changing the variable of υ_m to ρ_m and calculation of partial differential values in equation (41), enthalpy residual function becomes as follows:

$$h_m - h_{m,I} = -RT^2 \int_0^{\rho_m} \left(\frac{\partial Z}{\partial T}\right)_{\rho_m} \frac{d\rho_m}{\rho_m} + RT(Z-1) \tag{42}$$

Molar enthalpy for ideal gas could be calculated as follow:

$$h_{m,I} = \sum_{j=1}^{N} x_j {h_{m,i}}^j \tag{43}$$

where in equation (43), x_j is mole fraction of component j in mixture and $h^j_{m,I}$ is molar enthalpy for ideal gas and for component j in mixture.

$$h^j_{m,I} = h^j_{m,I0} + a_j T + b_j c_j \coth\left(\frac{c_j}{T}\right) - d_j e_j \tanh\left(\frac{e_j}{T}\right) \tag{44}$$

Coefficients in equation (44) are given in reference (DIPPR® 801, 2004). $h^j_{m,I0}$ is molar enthalpy for ideal gas of component J in mixture at reference state (25 °C,101.325 kPa).

The partial differential relations in equation (41) have been calculated using AGA8 EOS. Finally by integrations from equation (42) and computing ideal molar enthalpy using equation (44), molar enthalpy is calculated for natural gas. The enthalpy per unit mass then could be calculated as follows:

$$h = \frac{h_m}{M_w} \tag{45}$$

4. Numerical procedure

As explained previously, to calculate two independent thermodynamic properties, first law and conservation of mass equations are discretized as follow firstly (Farzaneh-Gord and Rahbari, 2012):

$$\frac{u_{cv}^{j+1} - u_{cv}^{j}}{\Delta\theta} = \frac{1}{m_{cv^j}}\left\{\left(\frac{\Delta Q_{cv}}{\Delta\theta}\right)^j + h_s^j\left(\frac{\Delta m_s}{\Delta\theta}\right)^j - P_{cv^j}\left(\frac{\Delta V}{\Delta\theta}\right)^j - h_d^j\left(\frac{\Delta m_d}{\Delta\theta}\right)^j - \left(\frac{\Delta m_{cv^j}}{\Delta\theta}\right)u^j\right\} \tag{46}$$

$$\frac{\Delta m_{cv}}{\Delta\theta}=\frac{\dot{m}_s-\dot{m}_d}{\omega}\Rightarrow m_{cv}^{j+1}-m_{cv}^{j}=\Delta\theta\left(\frac{\dot{m}_j^{s}-\dot{m}_d^{j}}{\omega}\right)\Rightarrow m_{cv}^{j+1}=m_{cv}^{j}+\Delta\theta\left(\frac{\dot{m}_s^{j}-\dot{m}_d^{j}}{\omega}\right) \tag{47}$$

And then specific internal energy and m_{cv} are computed from equations (46) and (47) for each crank angle by employing Runge–kotta method. Then density is calculated as below by knowing in-cylinder volume at each crank angle:

$$\rho_{(\theta)}^{j+1}=\frac{m_{cv(\theta)}^{j+1}}{V_{cv(\theta)}^{j+1}} \tag{48}$$

These two thermodynamic properties (density and specific internal energy) are enough to identify the other thermodynamic properties (temperature, pressure …). For calculating pressure and temperature for each time step, thermodynamic table which formed based on AGA8 EOS, are used. The table is arranged according to internal energy (u) and density ($\rho(\theta_i)$). Functions of pressure and temperature are prepared by Curve fitting method. This method is based on the study of Farzaneh-Gord and Rahbari (Farzaneh-Gord and Rahbari, 2011). They developed novel correlations for calculating natural gas thermodynamic properties. Their study shows that the correlations could predict natural gas properties with an error that is acceptable for most engineering applications. The range of pressure and temperature which the correlations have been developed for, are as follows: 0.2 < P(MPa) < 25; 250 < T(K) < 350. Based on these pressure and temperature range, the average absolute percent deviation (AAPD) for calculating natural gas thermodynamic properties is less than 3%. Details of the calculation method and error for curve fitting method are presented in Farzaneh-Gord and Rahbari (2011).

The values of work and indicated work per in-control volume mass are also calculated as following equations:

$$W=F\int_{Cycle(\theta=0\ to\theta=2\pi)}PdV=F\times\sum_{j=1}^{N}P^j dV^j=\int_{Cycle(\theta=0\ to\ \theta=2\pi)}PdV \tag{49}$$

$$W_{indicated}=\frac{1}{m_{cv}}\int_{Cycle(\theta=0\ to\ \theta=2\pi)}PdV=\frac{1}{m_{cv}}\sum_{j=1}^{N}P^j dV^j \tag{50}$$

In which N and F are the number of steps and the frequency respectively. Frequency could be obtained as:

$$F=2\pi\times\omega \tag{51}$$

5. Results and discussion

Firstly, for validation the mathematical method in this study, the results of numerical method have been compared with available experimental results. Venkatesan et al. (Farzaneh-Gord and Rahbari, 2011) measured in-control volume conditions variation in a single stage, single cylinder reciprocating compressor for air as the working fluid. Fig. 2 compares the variation of in-control volume pressure between numerical values and experimental result (Farzaneh-Gord and Rahbari, 2011) against crank angle. In the numerical study, the suction and discharge pressure assumed constant. In the experimented case, the volume displaced by the piston is larger than the amount of air entering into the cylinder during suction period. As a result for the experimented case, a decrease in cylinder pressure is expected. This could be seen in the figure. Similarly, the volume displaced by the piston is greater than the volume of air discharged through discharge port for the experimented case during discharge period. Therefore, an increase in cylinder pressure is expected. Also volume flow rate and peak pressure are compared in Table 2. Generally, there are a good agreement between the measured and numerical values.

The rest of the results presented in this study is for a compressor with following characteristics: $B = 14.5$ cm, $S = 10$ cm, $r_s = 2.96$ cm, $r_d = 4.33$ cm, $m_s = m_d = 0.02$ kg, $k_s = k_d = 16$N/mm and $T_s = 286$ K. The pressure of discharge plenum and also pressure ratio are considered to be 15 MPa and 5 respectively. The effects of various parameters are also investigated in separated sections.

5.1. *Effect of angular speed on compressor operation for real and ideal gas models*

In this section the effect of angular speed on compressor operation for real and ideal gas models are presented. For each models the investigated angular speeds are 500, 1000, and 1500 rad s^{-1}. The variation of in-control volume pressure and temperature against crank angle for ideal and real gas models are shown in Fig. 3(a) and (b). For these figures, the modeling begins from Top Dead Center (TDC) where cylinder volume is the same as clearance volume. With motion of piston from TDC towards bottom (the move towards Bottom Dead Center (BDC)), cylinder volume is increased and subsequently

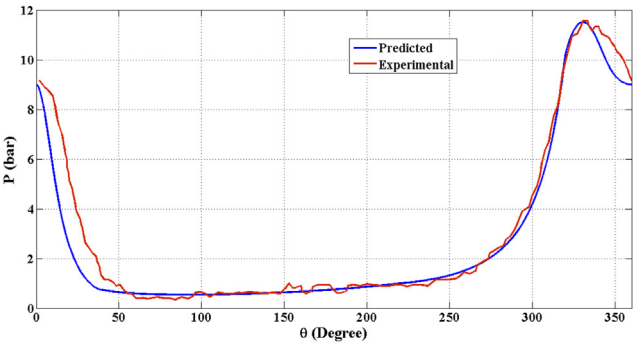

Fig. 2 – Comparison between numerical and measured values (Farzaneh-Gord and Rahbari, 2011) of cylinder pressure at $\omega = 1800$ rpm.

Table 2 – Comparison between measured (Farzaneh-Gord and Rahbari, 2011) and numerical value of two points pressure at $\omega = 1800$ rpm.

	Peak pressure (bar)	Free air delivered (liter min^{-1})
Experimental (Nagarajan et al., 2009)	11.58	277.4
Predicted	11.51	280.2
Error (%)	0.6	1.01

pressure and temperature are decreased. For all angular speeds, graphs are coincidence until suction valve is opened. Once suction valve is opened suction process starts. With increasing the angular speed, the in-control volume pressure decreases more sharply for each model (Fig. 3(a)). Because less time for heat lost in high angular speeds, the in–cylinder temperature reaches to higher values (see Fig. 3(b)). Consequently, if values angular speed is higher, the peak of in-control volume pressure has been increased. Also, there is a direct relation between increase in angular speed and rise in discharge temperature. For example, as angular speed increases from 500 to 1500 rad/s, the discharge temperature rises about 11.5 K and 8 K for ideal and real gas respectively. Furthermore, at the same angular speed the in-control volume temperature of ideal gas is higher than real gas temperature.

Once in-control volume pressure is lower than suction pressure as such that the force produced by the pressure difference is more than force of suction valve spring, suction valve will be opened. This causes natural gas flows through suction valve and enters into cylinder. Suction process continues until force due to pressure difference is balanced by the force of suction valve spring. Then around BDC, suction valve is closed. In BDC, piston motion is become backward and cylinder pressure and subsequently temperature is increased. When force due to pressure difference (in-control volume pressure and discharge pressure) is more than force due to discharge spring valve, discharge valve is opened. This causes that natural gas flows out through discharge valve. When piston reaches to the TDC, the compressor completes a whole cycle.

Fig. 4(a) and (b) show the effects of angular speeds on suction and discharge valves motion for real and ideal gas models. The figures illustrate that valves vibration happens at low crank angle. As the angular speed increases, the valves opening time increases.

Fig. 5 shows the effect of angular speeds on suction mass flow rate for real and ideal gas models. With opening suction valve, the values of mass flow rates become maximum quickly. Also the figure present that there is backward flow for

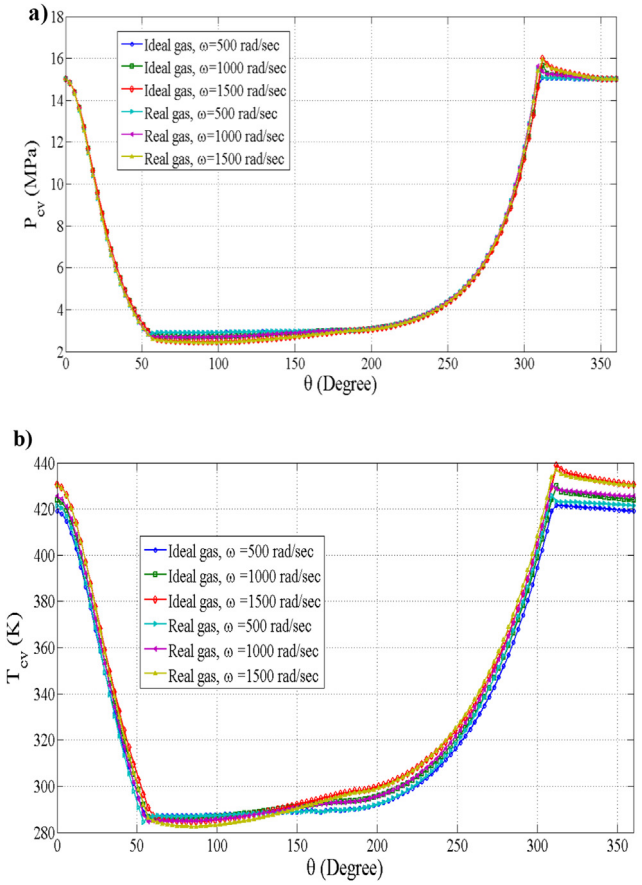

Fig. 3 – Variation of a) in–cylinder pressure and b) in–cylinder temperature vs. crank angle based on different angular speeds for ideal and real gas models.

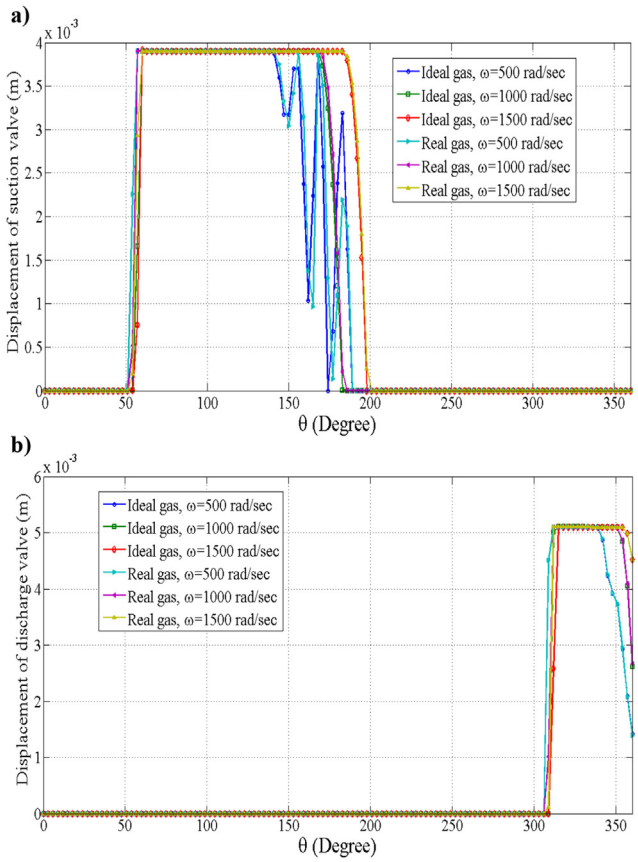

Fig. 4 – Variation of a) displacement of suction valve and b) discharge valve vs. crank angle based on different angular speeds for ideal and real gas models.

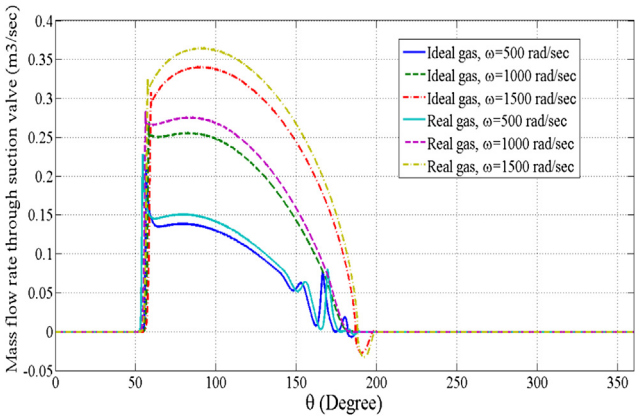

Fig. 5 – Variation of suction mass flow rate vs. crank angle based on different angular speeds for ideal and real gas models.

suction valve. As the angular speed increases, the valves opening time increases.

Fig. 6(a) and (b) present the mass flow rate and work for real and ideal natural gas models respectively. Based on these figures, as angular speed increases, the number of cycles is done by compressor in specific time increases too, therefore the mass flow rate and work will be increased. As the density of the gas is higher for real gas comparing to the ideal gas model, the mass flow rate that entering control volume is higher for real gas model, consequently, in-cylinder gas is higher for real gas model. Higher in-cylinder mass needs more compressing power which makes the consuming work to be higher in real gas model comparing to ideal one.

5.2. *Effect of clearance value on compressor operation for real and ideal gas models*

Due to different reasons such as the heat expansion of compressor pieces, exist of clearance in reciprocating compressor which is unavoidable. The effect of clearance values on performance compressor, percent of clearances 7, 11 and 15, have been investigated. Fig. 7(a) and (b) present the variation of in-control volume pressure and temperature verse to various clearance percentages, for real and ideal gas models respectively. As it is shown, the lines of pressure in suction and discharge processes are almost coincidence. Fig. 7(b) illustrates that the effect of clearance value on discharge temperature isn't much. For example, temperature difference of discharge gas between clearances 7% and 15% is about 1.5 K for real or ideal gas models. As clearance decreases, the temperature of expanded gas is decreased. As an example, temperature difference of expanded gas between clearances 7% and 15% just before suction process is 2.5 K.

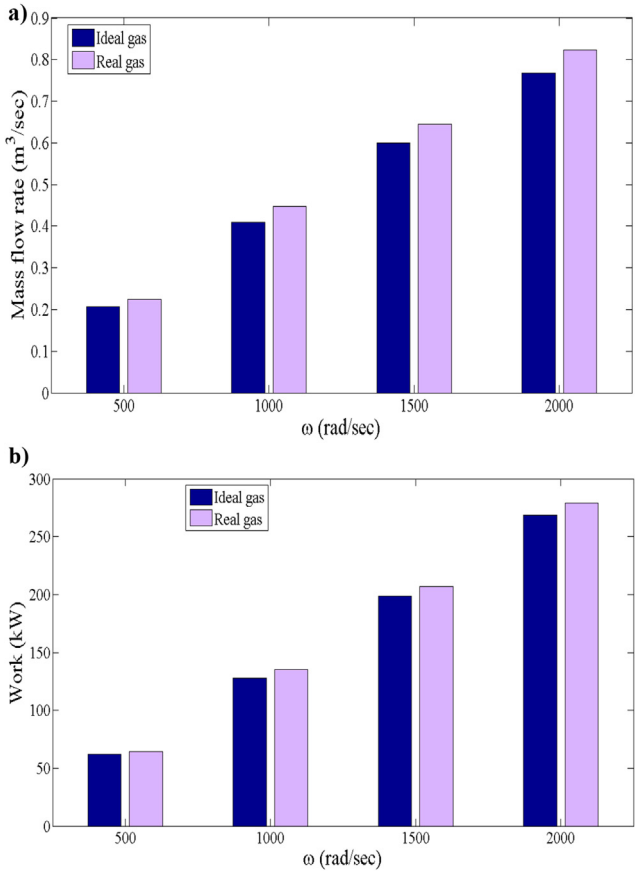

Fig. 6 – Variation of a) Mass flow rate and b) work for various angular speeds for ideal and real gas models.

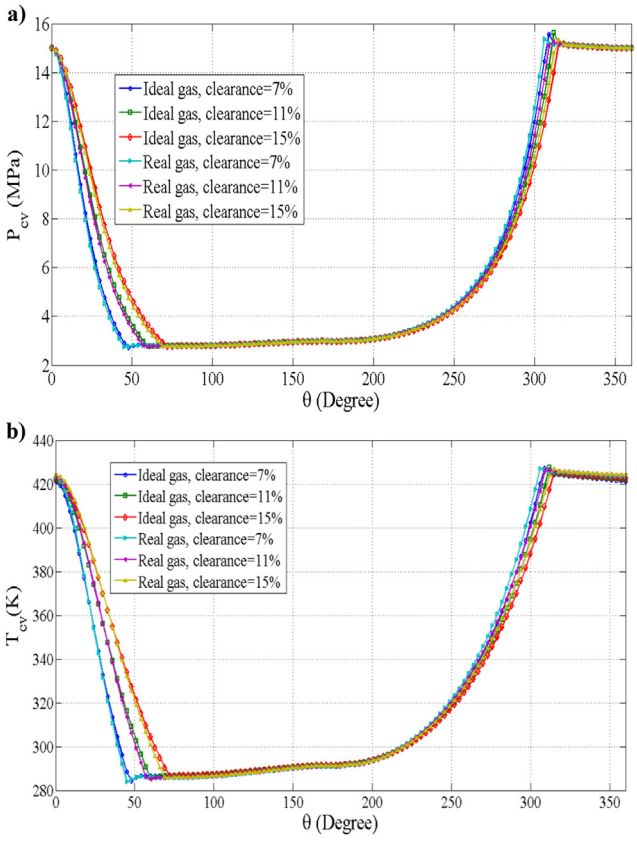

Fig. 7 – Variation of a) in-control volume pressure and b) in-control volume temperature vs. crank angle based on various clearances for ideal and real gas models.

Fig. 8 shows displacements of suction and discharge valves according crank angle based on various clearances for ideal and real gas models. With decreasing clearance, expansion process ended faster and suction valve is opened sooner (Fig. 8(a)). Values of clearance influenced on compression process, as with decreasing clearance values the compression process ended faster and discharge valve is opened sooner (Fig. 8(b)).

Fig. 9 presents the variations of suction mass flow rates against crank angle based on various clearances for ideal and real gas models. As noted above, in suction valve the backward flow occurs.

Bar charts of mass flow rate and work based on different clearances for ideal and real gas models are shown in Fig. 10 (a) and Fig. 10 (b) respectively. As shown these figures, the mass flow rate and work in same clearance for real gas model is greater than ideal gas model.

Fig. 11 shows the indicated work that natural gas received in various clearances for ideal and real gas models. Based on this figure, when clearance is increased, the work per mass is also increased. Also, the result illustrates that change in clearance doesn't much effect on indicated work in both gas models. Also, based on Fig. 11, the indicated work required for compressing a given value of natural gas for ideal gas model is more than indicated work required for real gas model. As the indicated work is calculated by dividing work to one cycle mass flow rate, The indicated work in real gas model is slightly higher than the ideal gas model.

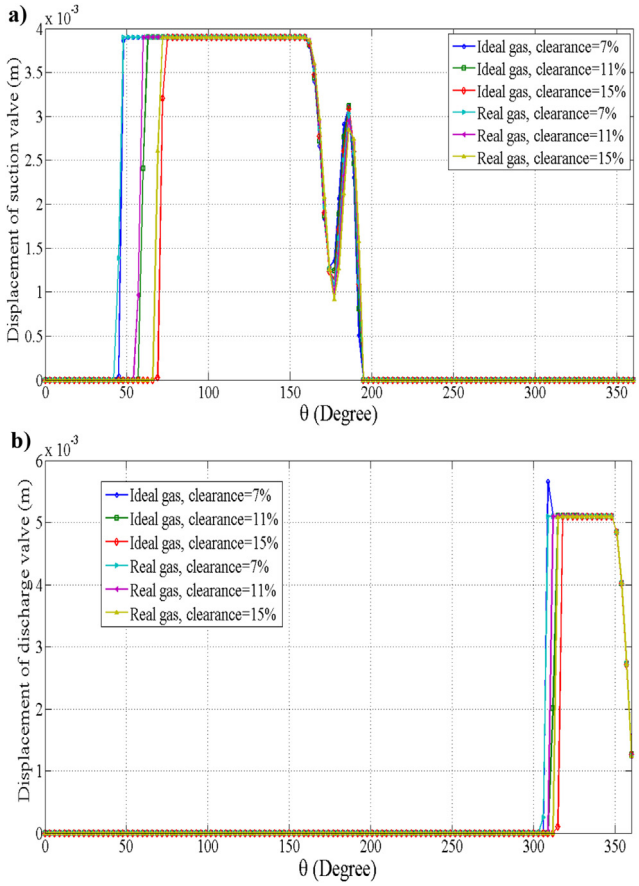

Fig. 8 – Displacement of a) suction valve and (b) discharge valve vs. crank angle based on various clearances for ideal and real gas models.

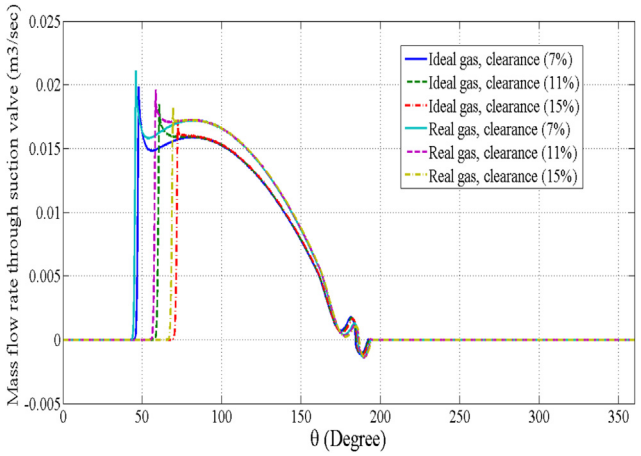

Fig. 9 – Variation of suction mass flow rate vs. crank angle based on different clearances for ideal and real gas models.

5.3. *Effect of pressure ratio on compressor operation for real and ideal gas models*

In this section the effects of pressure ratio on compressor performance for real and ideal gas models have been studied.

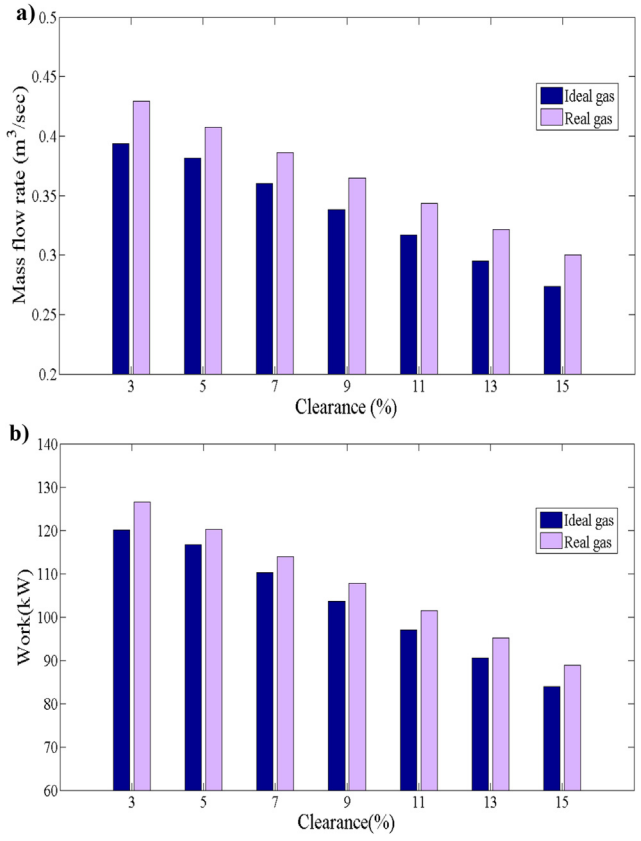

Fig. 10 – Variation of a) Mass flow rate b) work based on different clearances for ideal and real gas models.

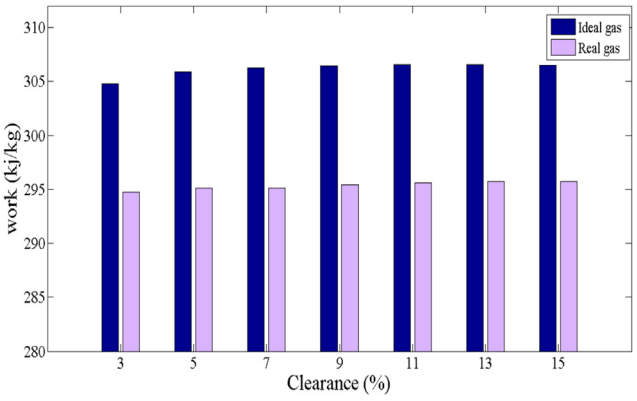

Fig. 11 – Variation if indicated work for various clearances for ideal and real gas models.

Fig. 12 (a) and (b) show effects of pressure ratio on mass flow rate and work respectively. The effect of pressure ratio is done for both real and ideal gas models. According to Fig. 12, as pressure ratios increases, mass flow rate and subsequently work are reduced for both real and ideal gas models.

Fig. 13 shows the indicated work for various pressure ratios. According to Fig. 13, as pressure ratio increases, the work required for compressing unit mass increased for both real and ideal gas assumptions. Based on this figure, the indicated work that required for compression in ideal gas model is more than real gas model.

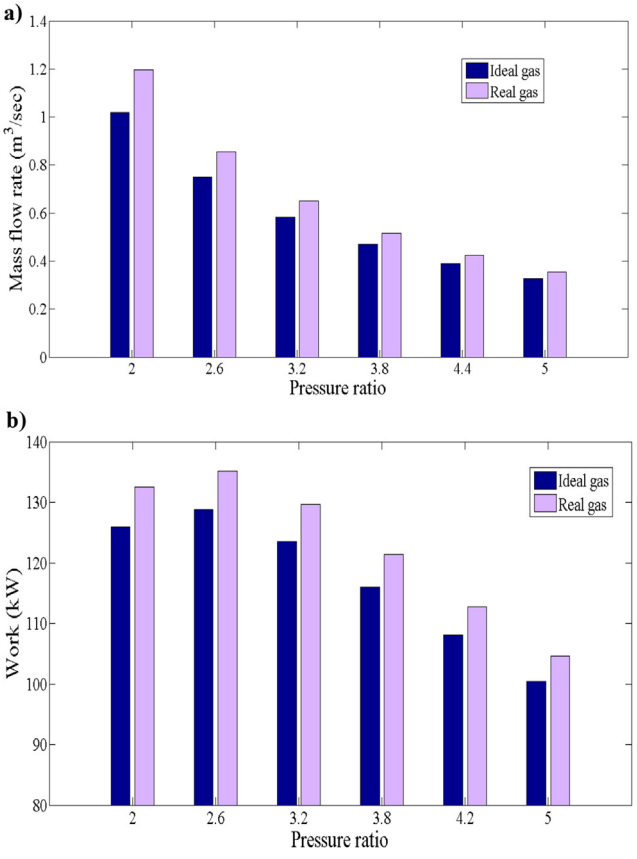

Fig. 12 – Variation of a) Mass flow rate and b) work for various pressure ratios for ideal and real gas models.

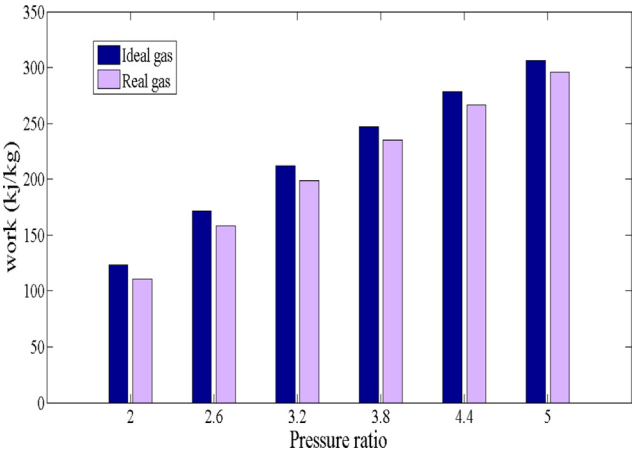

Fig. 13 – Variation of indicated work for various pressure ratios for ideal and real gas models.

6. Conclusion

Reciprocating compressors are used extensively in industry due to their ability to high pressure ratio achievement. One of the most important applications of these compressors is in CNG fueling station. Comprehension the demeanor of the reciprocating compressors and investigating influences of different parameters are fascinating topics. The numerical simulating is proved to be an effective tool to investigate performance of these compressors based on ideal and real gas models.

The first law of thermodynamics and mass balance equation has been used as theoretical tools to study performance of one stage CNG reciprocating compressors. For real gas model, the required thermodynamic properties of natural gas, as fluid working, have been computed using AGA8 Equation of State (EOS) and thermodynamics relationships. For real and ideal gas models, the simulation predicted in-control volume pressure and temperature and valves motions for various crank angles. The mass flow rate, work and indicated work are also calculated. The results from the presented model have been validated against the previous measured values and good agreement has been obtained. The effects of different parameters on the performance of the compressors as angular speed, clearance and pressure ratio have been studied.

The results show that for ideal and real gas models, as angular speed increases, the in-control volume temperature increases too. The valves vibration occurs at low crank angle and as the angular speed increases, the valves opening angle increases. There is backward flow for suction valve during each cycle. Clearance value doesn't much effect on indicated work and so necessary work for compressing a given value of gas in various clearances is almost fixed.

The results also show as pressure ratio increases, the mass flow rate and subsequently work are reduced for both real and ideal gas models, while indicated work per unit mass increases.

Based on results, in same condition, (identical angular speed, clearance and pressure ratio) the in-control volume temperature for ideal gas model is more than real gas models. Also the mass flow rate and work for real gas model, is greater

than ideal gas model. On the other hand, the indicated work that required for compression in ideal gas model is higher than real gas model.

Acknowledgment

Authors would like to thank the officials in NIOPDC Company for financial support.

REFERENCES

AGA8-DC92 EoS, 1992. Compressibility and Super Compressibility for Natural Gas and Other Hydrocarbon Gases. Transmission Measurement Committee, Arlington, VA. Report No. 8, AGACatalog No. XQ 1285.

Adair, R.P., Qvale, E.B., Pearson, J.T., 1972. Instantaneous heat transfer to the cylinder wall in reciprocating compressors. In: Purdue Compressor Technology Conference Proc, pp. 521–526.

Aprea, C., Mastrullo, R., Renno, C., 2009. Determination of the compressor optimal working conditions. Appl. Therm. Eng. 29, 1991–1997.

Bin, Tang, Yuanyang, Zhao, Liansheng, Li, Guangbin, Liu, Le, Wang, Qicha, Yang, et al., 2013. Thermal performance analysis of reciprocating compressor with stepless capacity control system. Appl. Therm. Eng. 54, 380–386.

Boswirth, L., 1980. Flow forces and the tilting of spring loaded valve plates. In: Proceedings of the Purdue Compressor Conference, pp. 185–197.

Brablik, J., 1972. Gas pulsations as a factor affecting operation of automatic valves in reciprocating compressors. In: Proceeding of Purdue Compressor Technology Conference, pp. 188–195.

Castaing-Lasvignottes, J., Gibout, S., 2010. Dynamic simulation of reciprocating refrigeration compressors and experimental validation. Int. J. Refrigeration 33, 381–389.

Cezar, O.R. Negrao, Erthal, Raul H., Andrade, Diogo E.V., da Silva, Luciana Wasnievski, 2011. A semi- empirical model for the unsteady-state simulation of reciprocating compressors for household refrigeration applications. Appl. Therm. Eng. 31, 1114–1124.

DIPPR® 801, 2004. Evaluated Standard Thermophysical Property Values. Design Institute for Physical Properties. Sponsored by AIChE.

Da Riva, Enrico, Del Col, David, 2011. Performance of a semi-hermetic reciprocating compressor with propane and mineral oil. Int. J. Refrigeration 34, 752–763.

Damle, R., Rigola, J., Perez-Segarra, Castro, J., Oliva, A., 2011. Object-oriented simulation of reciprocating compressors: numerical verification and experimental comparison. Int. J. Refrigeration 34, 1989–1998.

Elhaji, M., Gu, F., Ball, A.D., Albarbar, A., 2008. Numerical simulation and experimental study of a two-stage reciprocating compressor for condition monitoring. Mech. Syst. Signal Process. 22, 374–389.

Farzaneh Gord, M., Niazmand, A., Deymi-DashteBayaz, M., 2013. Optimizing reciprocating air compressor design parameters based on first law analysis. U.P.B. Sci. Bull. Ser. D. 75 (4).

Farzaneh-Gord, Mahmood, Rahbari, Hamid Reza, 2011. Developing novel correlations for calculating natural gas thermodynamic properties. Chem. Process Eng. 32 (4), 435–452.

Farzaneh-Gord, M., Rahbari, H.R., 2012. Numerical procedures for natural gas accurate thermodynamics properties calculation. J. Eng. Thermophys. 21 (4), 213–234.

Farzaneh-Gord, M., Khamforoush, A., Hashemi, Sh, Pourkhadem Namin, H., 2010. Computing thermal properties of natural gas by utilizing AGA8 equation of state. Int. J. Chem. Eng. Appl. 1 (1), 20–24.

Farzaneh-Gord, M., Deymi-Dashtebayaz, M., Rahbari, H.R., 2012. Optimising compressed natural gas filling stations reservoir pressure based on thermodynamic analysis. Int. J. Exergy 10 (3), 299–320.

Farzaneh-Gord, M., Rahbari, H.R., Deymi-Dashtebayaz, M., 2014. Effects of natural Gas compositions on CNG fast filling process for buffer storage system. Oil Gas Sci. Technol. e Rev. IFP Energies nouv. 69 (2), 319–330.

ISO-12213-2, 1997. Natural Gas Calculation of Compression Factor-Part 2: Calculation Using Molar-composition Analysis. ISO, Ref. No. ISO- 12213-2:1997(E).

Lee, Sukhyung, 1983. First Law Analysis of Unsteady Processes with Application to a Charging Process and a Reciprocating Compressor. A Thesis presented in Partial Fulfillment of the Requirements for Degree of master Science. The Ohaio state University.

Link, Rodrigo, Deschamps, Cesar J., 2011. Numerical modeling of startup and shutdown transients in reciprocating compressors. Int. J. Refrigeration 34, 1398–1414.

Ma, Yuan, He, Zhilong, Peng, Xueyuan, Xing, Ziwen, 2012. Experimental investigation of the discharge valve dynamics in a reciprocating compressor for trans-critical CO_2 refrigeration cycle. Appl. Therm. Eng. 32, 13–21.

Maríc, I., 2005. The Joule–Thomson effect in natural gas flow-rate measurements. Flow. Meas. Instrum. 16 (2), 387–395.

Maríc, I., 2007. A procedure for the calculation of the natural gas molar heat capacity, the isentropic exponent, and the Joule–Thomson coefficient. Flow. Meas. Instrum. 18 (1), 18–26.

Maríc, I., Galovic, A., Smuc, T., 2005. Calculation of natural gas isentropic exponent. Flow. Meas. Instrum. 16 (1), 13–20.

McGovern, J.A., Harte, S., 1995. An exergy method for compressor performance analysis. Int. J. Refrigeration 18 (6), 421–433.

Moran, M.J., Shapiro, H.N., 2007. Fundamentals of Engineering Thermodynamics, sixth ed. Wiley, ISBN 0471787353.

Morriesen, A., Deschamps, C.J., 2012. Experimental investigation of transient fluid flow and superheating in the suction chamber of a refrigeration reciprocating compressor. Appl. Therm. Eng. 41, 61–70.

Nagarajan, Govindan, Venkatesan, Jayaraman, Seeniraj Retteripatti, Venkatasamy, Murugan, Ramasamy, 2009. Mathematical modeling and simulation of a reed. Therm. Sci. 13 (3), 47–58.

Ndiaye, D., Bernier, M., 2010. Dynamic model of a hermetic reciprocating compressor in on-off cycling operation (Abbreviation: compressor dynamic model). Appl. Therm. Eng. 30, 792–799.

Perez-Segarra, C.D., Rigola, J., Soria, M., Oliva, A., 2005. Detailed thermodynamic characterization of hermetic reciprocating compressors. Int. J. Refrigeration 28, 579–593.

Richard, Stone, 1999. Introduction to Internal Combustion Engines. Department of Engineering Science, University of Oxford.

Singh, R., 1975. Modeling of Multi Cylinder Compressor Discharge Systems. PhD thesis. Purdue University.

Stouffs, P., Tazerout, M., Wauters, P., 2000. Thermodynamic analysis of reciprocating compressors. Int. J. Thermodyn. Sci. 40, 52–66.

Winandy, E., Saavedra, O., Lebrun, J., 2002. Simplified modeling of an open-type reciprocating compressor. Int. J. Sci. 41, 183–192.

Yang, Bin, Bradshaw, Craig R., Groll, Eckhard A., 2012. Modeling of a semi-hermetic CO_2 reciprocating compressor including lubrication submodels for piston rings and bearings. Int. J. Refrigeration XXX, 1–13.